Sensors & Actuators: B. Chemical 346 (2021) 130590

Contents lists available at ScienceDirect

Sensors and Actuators: B. Chemical

journal homepage: www.elsevier.com/locate/snb

Transformer oil-dissolved acetylene detection with photonic crystal fiber loop ringdown spectroscopy

Yuan Wang [a], Guo-ming Ma [a,*], Diya Zheng [a], Wei-qi Qin [a], Jun Jiang [b], Hong-yang Zhou [c], Chao Yan [d]

[a] State Key Laboratory of Alternate Electrical Power System with Renewable Energy Sources, North China Electric Power University, Beijing, 102206, PR China
[b] Center for More-Electric-Aircraft Power System, Nanjing University of Aeronautics and Astronautics, No. 169 Sheng Tai West Road, Nanjing, 211106, PR China
[c] Guangdong Engineering Technology Research Centre of Power Equipment Reliability in Complicated Coastal Environments, Tsinghua Shenzhen International Graduate School, Tsinghua University, Shenzhen, Guangdong, 518055, PR China
[d] Department of Mechanical and Aerospace Engineering, Princeton University, Princeton, NJ, 08544, United States

ARTICLE INFO

Keywords:
Power transformer
Dissolved gas analysis
Acetylene
Photonic crystal fiber
Focused ion beam
Fiber loop ringdown spectroscopy

ABSTRACT

When faults happen in a power transformer, a variety of small-molecular gases will generate and dissolve in transformer oil. Therefore, dissolved gas analysis is one of the important methods to monitor the operating status of transformers. This paper proposes an optical acetylene sensing method based on hollow core photonic crystal fiber (HC-PCF) and fiber loop ringdown spectroscopy (FLRDS). Focused ion beam technique is used to complete the processing of micro-sized channels along a HC-PCF. It takes about 11 min to fully fill the entire length of a 0.83 m HC-PCF with acetylene. Furthermore, the FLRDS system based on the dual-wavelength method achieves a minimum detection limit of 0.71 ppm. This detection system improves detection stability and provides a new idea for online monitoring of dissolved gases in transformer oil.

1. Introduction

Large power transformers (LPTs) play an important role in the high-voltage power system. The long-term safe operation of LPTs is very important since any failures of LPTs might induce a serious blackout [1]. Hence, it is necessary to develop online monitoring tools to monitor the operation status of LPTs effectively. When faults occur in LPTs, small amount of transformer oil will be decomposed into trace gases (such as H_2, C_2H_2, CH_4, etc.), and such gases will be dissolved in the oil. By monitoring the composition and the concentration of oil-dissolved gases, it is possible to figure out whether there are any early latent faults and the severity of faults inside LPTs in time.

Traditionally, gas chromatography (GC) is one of the most used methods for dissolved gas analysis (DGA). For off-line GC, detection is usually performed every 12 months [2,3], and it is hard to figure out latent faults in time. For on-line GC, detection is performed every 24 h, which solves the above problem to a certain extent. However, when a fault occurs in the transformer tank far away from the oil extraction port, it takes a long time for the small molecule gas dissolved in the transformer oil to diffuse to the oil extraction port. This process may take dozens of hours, which is not conducive to the rapid detection of changes in gas content and composition by online GC equipment, and it is difficult to find out possible faults in time. What is more, GC still has some problems, such as easy contamination of the chromatographic column and the need to consume carrier gas, which are inconvenient for actual application and results in high application cost [4,5].

Recently, the development of ultra-high sensitivity optical gas sensors for in-situ online monitoring has become a research hotspot. Infrared absorption spectroscopy is a commonly applied sensing technique [1,6,7]. It distinguishes gas compositions by different gas molecules having different absorption lines and distinguishes gas concentration by measuring the magnitude of absorption. In addition, the minimum detection limit (MDL) is proportional to the absorption pathlength. Q.X. He et al. used a 20 cm-long open-reflective gas-sensing probe to detect acetylene, and the MDL reached 8.69 ppm [8]. However, the acetylene concentration for transformers working in caution state is 2~9 ppm [2], which is lower than the MDL reported by the above literature. In order to achieve a better performance in MDL, researchers have conducted a lot of research on how to increase the optical absorption pathlength. G.M. Ma et al. introduced a tunable diode laser absorption spectroscopy (TDLAS) system for acetylene sensing with a Herriott cell, and a MDL of 0.63 ppm was achieved [9]. A Herriott cell is made up of two opposing spherical mirrors, which allows the laser

* Corresponding author.
E-mail address: ncepumgm@ncepu.edu.cn (G.-m. Ma).

https://doi.org/10.1016/j.snb.2021.130590
Received 20 May 2021; Received in revised form 19 July 2021; Accepted 6 August 2021
Available online 10 August 2021

Nomenclature

List of abbreviation

LPTs	Large power transformers
FIB	Focused ion beam
MDL	Minimum detection limit
GC	Gas chromatography
TLS	Tunable laser source
AOM	Acoustic optical modulator
OSC	Oscilloscope
HC-PCF	Hollow core photonic crystal fiber
FLRDS	Fiber loop ringdown spectroscopy
DGA	Dissolved gas analysis
CRDS	Cavity ringdown spectroscopy
PD	Photodetector
BPD	Balanced photodetector

Symbols

λ	Light wavelength
I	Transmitted light intensity
C	Gas concentration
C_0	Initial acetylene concentration in gas chamber
D	Acetylene diffusion coefficient
σ	Standard deviation
I_0	Incident light intensity
α	Absorption coefficient
L	Absorption pathlength
C_t	Acetylene concentration in HC-PCF
G	Gain of amplifier

travels multiple times in it and enables a long absorption pathlength. However, Herriott cell has a complicated structure and requires optical calibration before using every time, which is not suitable for on-line monitoring. What is more, the accuracy and the sensitivity of a sensing systems based on traditional infrared absorption spectroscopy is sensitive to fluctuations in light intensity [10–12]. This characteristic puts forward higher requirements on the detection environment and optical equipment.

Cavity ringdown spectroscopy (CRDS) provides new ideas for solving the above problems. CRDS was first proposed by A. O'Keefe and D.A.G. Deacon in 1988 [13]. Light will propagate several times in a gas cell, and the absorption pathlength will increase several times in turn. Unlike traditional infrared absorption spectroscopy that directly measures the attenuation of light intensity, CRDS measures the attenuation rate of light intensity to figure out the gas concentration. However, conventional CRDS needs to be optically calibrated before each detection due to the existence of cavity coupling optics and high reflectivity optical mirrors, the operation is complicated. In order to further simplify the gas sensing system, G. Stewart et al. demonstrated fiber loop ringdown spectroscopy (FLRDS) in 2001 [14]. In a FLRDS system, a fiber loop plays the role of the optic mirrors in CRDS. Furthermore, since long fibers can be coiled into small diameters, the entire system can be kept compact in size. Y. Zhao et al. presented a FLRDS-based acetylene sensor, and the effective optical pathlength of the gas cell was 25 cm [15]. Acetylene gas samples with concentrations from 0–5‰ were measured. Q.D. Zhang et al. [16] placed a photoacoustic spectroscopy gas cell (absorption pathlength was 3.4 cm) inside a fiber-optic ring cavity, and the MDL was 8.4 ppm for acetylene. This technique provides an important reference for the sensing of trace acetylene dissolved in transformer oil. However, for ensuring the compactness and ease of use of the FLRDS system, the effective optical pathlength of the gas cells used is relatively small currently. Therefore, the effective optical pathlength of the gas cell needs to be further lengthened to realize the detection of dissolved gas in transformer oil.

To simplify the operation while increasing the absorption pathlength, researchers have conducted gas sensing studies based on a hollow core photonic crystal fiber (HC-PCF). The core region of a HC-PCF can be used as a gas cell, and a long HC-PCF can be coiled into a small diameter which ensures a compact size. Y.L. Hoo et al. realized a MDL of 647 ppm for methane sensing with a 7 cm-long HC-PCF [17]. For better performance in MDL, one possible solution is to increase the length of the HC-PCF, but this will increase the time required for acetylene to diffuse into the hollow core of the HC-PCF and will seriously affect the real-time detection. W. Jin et al. presented a novel gas cell made with a piece of HC-PCF sandwiched by two single mode fibers with mirrored ends [18,19]. The absorption pathlength was lengthened by multiple times traveling in the fiber cavity. But dielectric mirrors are difficult to manufacture, and the cost is high. The FLRDS system can effectively solve the above-mentioned HC-PCF application problems.

In this paper, the gas diffusion process is studied, and a side-opening processing method for accelerating gas diffusion is proposed. Furthermore, this paper designs a FLRDS system suitable for the detection of dissolved acetylene in transformer oil, and carries out trace acetylene detection, which proves the superiority of the proposed system and its good performance.

2. Measurement principles

For a FLRDS gas sensing system, the concentration is obtained by calculating the ringdown time. A typical structure of FLRDS system is shown in Fig. 1(a). The input pulses propagate in an optical fiber loop consists of single mode fibers (SMF), a gas cell and an optical fiber coupler. In a FLRDS system, the input pulses enter and circulate in the fiber loop for several times. A decaying pulse train, shown in Fig. 1(b), will be coupled out and collected by a photodetector (PD) and then used for the derivation of gas concentration.

Defining δ is the total round-trip loss, the relationship between the intensity of the input light I_0 and the intensity of light I after passing through the fiber loop once could be given by [20]

$$I = I_0 e^{-\frac{\delta}{10\lg e}} \tag{1}$$

The intensity of the light propagates in the fiber loop for m times could be written into [21,22]:

$$I^m = I_0 e^{-\frac{m\delta}{10\lg e}} \approx I_0 e^{-\frac{m\delta}{4.34}} = I_0 e^{-\frac{\delta t}{4.34\tau}} = I_0 e^{-\frac{m\delta t_r}{4.34\tau}} \tag{2}$$

Where, t_r is the round-trip time and τ is the ringdown time when the pulse's intensity decays to 1/e of the initial.

Therefore, the optical pulse sequence detected by the photodetector decay exponentially, and δ could be expressed as:

$$\delta = \delta_0 + \delta_{gas} = \frac{4.34 t_r}{\tau} \tag{3}$$

Where δ_0 is inherent loss of the fiber loop, and δ_{gas} is gas absorption loss.

However, the inherent loss δ_0 is not constant during the detection process, because some external factors (such as tension, pressure, distortion, etc.) will change its magnitude. The dual-wavelength method can effectively solve this problem [23]. Two lasers with different wavelengths will be used for gas detection. The wavelength λ_1 is located at the strongest absorption line of the target gas, and the wavelength λ_2 is not covered with any absorption lines. When a narrow linewidth laser pulse of wavelength λ_1 enters the fiber loop, light will get absorbed by gas partially. Therefore, the round-trip loss $\delta(\lambda_1)$ contains the gas absorption loss and the inherent loss. However, a narrow linewidth laser

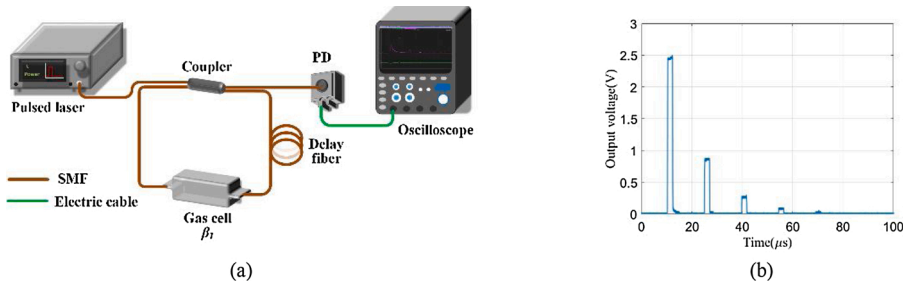

Fig. 1. (a) Schematic diagram of a FLRDS sensing system, (b) typical ringdown signal.

pulse of wavelength λ_2 will not get absorbed by the gas, the round-trip loss $\delta(\lambda_2)$ is equal to the inherent loss. Besides, the wavelengths λ_1 and λ_2 are almost equal and the two detections are performed almost simultaneously, so the inherent losses at the two wavelengths are almost equal to each other. Therefore, the gas absorption loss δ_{gas} could be written into [20,24,25]

$$\delta_{gas} = \delta(\lambda_1) - \delta(\lambda_2) = 4.34 t_r \left(\frac{1}{\tau(\lambda_1)} - \frac{1}{\tau(\lambda_2)} \right) \tag{4}$$

By adopting this method, the influence of inherent loss changes on the sensing results can be effectively suppressed. Moreover, according to the Beer-Lambert Law, the gas absorption loss could be further expressed as

$$\delta_{gas} = 4.34 \alpha(\lambda_1) L C \tag{5}$$

Where $\alpha(\lambda_1)$ is the gas absorption coefficient at wavelength λ_1, L is the absorption pathlength, C is the concentration of target gas. And then the concentration of target gas can be calculated by

$$C = \frac{\delta_{gas}}{4.34 \alpha(\lambda_1) L} = \frac{t_r}{\alpha(\lambda_1) L} \left(\frac{1}{\tau(\lambda_1)} - \frac{1}{\tau(\lambda_2)} \right) \tag{6}$$

3. Gas diffusion

3.1. Theoretical calculation

According to the Beer-Lambert law, change in light intensity caused by the target gas is proportional to the effective absorption pathlength. Therefore, the longer the effective absorption path of the gas cell, the lower the MDL of the system. The HC-PCF has the characteristics of easy to be coiled and can be used as an absorption gas cell with a small volume and a long optical pathlength. However, one of the main factors limiting the length of a HC-PCF is the long time required for gas to diffuse into the hollow core region, which seriously affects the response time of the sensing system. Assuming that the outside of the HC-PCF is at around atmospheric pressure, and the gas flows into the core region from the two ends of the HC-PCF without pressurizing, the relationship between the relative concentration inside and outside the core region C_t/C_0 over time can be expressed as [26–28]:

$$\frac{C_t}{C_0} = 1 - \frac{8}{\pi^2} \sum_{n=0}^{\infty} \frac{1}{(2n+1)^2} \exp\left[- \frac{(2n+1)^2 \pi^2}{L^2} D \cdot t \right] \tag{7}$$

Where C_0 is the initial acetylene concentration in gas chamber, mol/L; C_t is acetylene concentration in the hollow core region of a HC-PCF, mol/L; L is the length of HC-PCF, m; t is the gas diffusion time, s; D is the acetylene diffusion coefficient, which is about 1.8×10^{-5} $m^2 s^{-1}$.

This paper defines that when C_t is equal to 90 % of C_0, the gas diffusion reaches a steady flow state, and then the corresponding time is named as the gas diffusion saturation time. According to Ref. [17], in the detection of trace acetylene based on direct absorption spectroscopy using HC-PCF as a gas cell, the absorption pathlength needs to be at least 3 m. If a 3-meter-long HC-PCF is used directly, and the gas diffusion saturation time is about 29.47 h. A gas diffusion saturation time of tens of hours is extremely undesirable for real-time gas monitoring.

However, when the FLRDS system is used, the length of the HC-PCF can be shortened. Considering the connection loss between the HC-PCF and the SMF and the coupling loss introduced by the coupler and other inherent losses, the photodetector can only collect 3–4 effective ringdown pulses as usual [29]. Assuming that 3 effective ringdown pulses are collected, only 1 m-long HC-PCF can achieve an absorption pathlength of 3 m. In this case the gas diffusion saturation time is greatly shortened to 3.47 h. Fig. 2 shows the relationship between the gas diffusion time and relative gas concentration of two different length HC-PCFs with two ends open to atmospheric pressure.

3.2. Microstructure processing

In order to further shorten the gas diffusion saturation time, one possible solution is to fabricate multiple micro-structured side-openings along a HC-PCF. With the rapid developments in microelectronics technology, focused ion beam (FIB) processing technique becomes more mature and reliable than femtosecond laser processing technique [30–32]. The advantage of FIB technology is that it can achieve micro-processing with sub-micron spatial resolution and a better surface finish than femtosecond laser processing technique. Different from the irregular structure of the microchannel processed by the femtosecond laser technique, the microchannel processed by the FIB is smoother and more regular, leaving no undesirable particles. Moreover, the dual-beam instruments that combine scanning electron microscope (SEM) and FIB are commercially available nowadays. Therefore, FIB has a strong potential in fiber microstructure processing applications.

In this paper, a Strata 400S FIB (Thermo Fisher Scientific) with Ga^+ ion source was used to drill micro-channels for gas diffusion. The principle of FIB processing is shown in Fig. 3(a). The core diameter of HC-

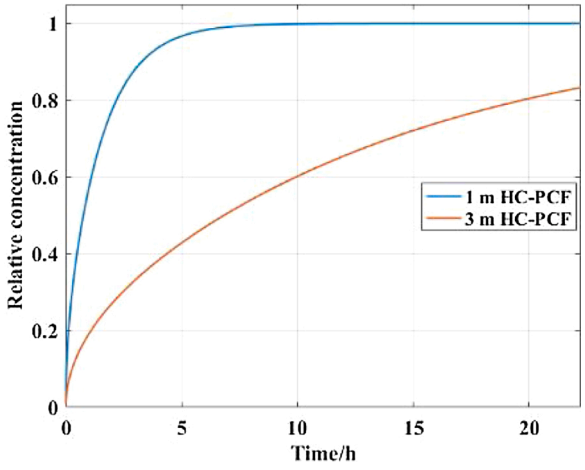

Fig. 2. Relationship between gas diffusion time and relative gas concentration inside different lengths of HC-PCFs.

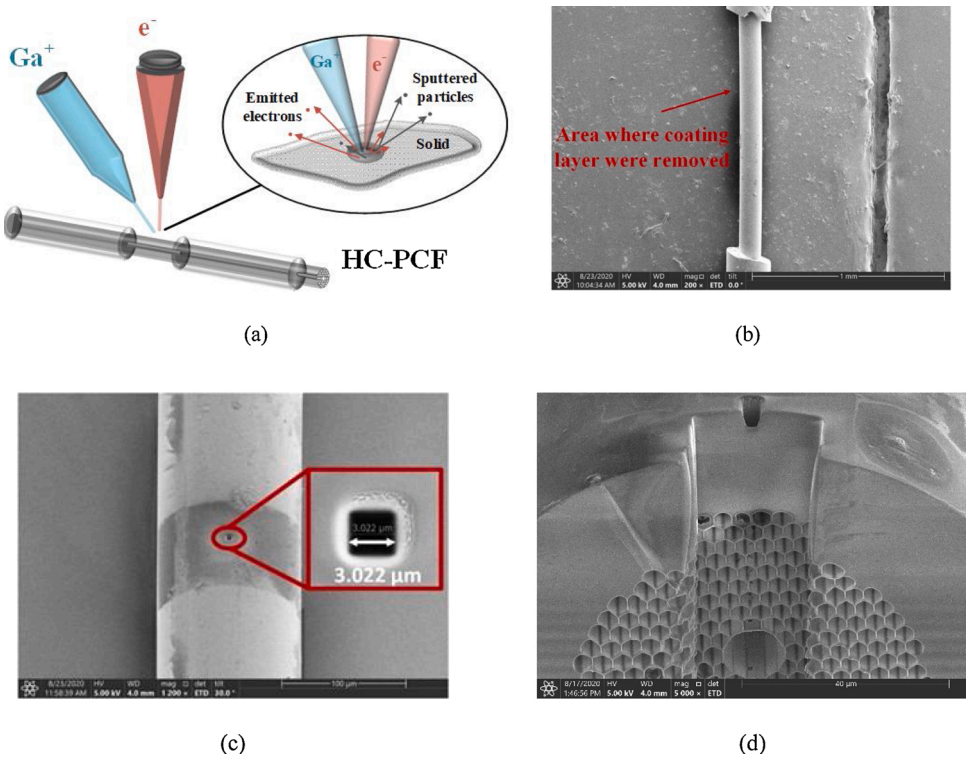

Fig. 3. (a) Schematic diagram of FIB, (b) SEM image of a HC-PCF before FIB milling (part of coating layer were removed), (c) processed HC-PCF with a micro-structured side-opening, (d) internal image of a HC-PCF after milling.

PCF (NKT Photonics, HC-1550-02) is about 10 μm, and cladding diameter is about 120 μm. Although FIB is a powerful microstructure processing tools, it is still not easy to precisely drill microchannels on the side of a PCF due to its thick acrylate polymer coating (coating diameter is about 220 μm). Therefore, the coating layer on the surface of HC-PCF needs to be removed before FIB processing as shown in Fig. 3(b). Then the processed HC-PCF is fixed on the top of conductive carbon tape which is attached to a silicon board. In addition, a thin layer of gold was deposited on the surface of HC-PCF for dissipating the excess charges.

Because the diameter, and number of the microchannels along the HC-PCF will affect the gas diffusion saturation time and the transmission loss, it will affect the response time and detection performance of the HC-PCF-based gas sensor in turn. Therefore, to reduce the transmission loss caused by the large-diameter microchannels and achieve the fast-response detection, this paper chose to process the microchannels with the smallest diameter possible on the surface of the HC-PCF, while increasing the number of microchannels to ensure the effective shortening of the gas diffusion saturation time. This paper used FIB technique to process microchannels along a HC-PCF, and finally determined the corresponding FIB processing parameters that ensuring size of the microchannel (X × Y×Z) was set to be 3 μm × 3 μm × 60 μm. The FIB milling was conducted with a high voltage of 30 kV and a beam current of 2.5 nA. Based on this processing parameter, microchannels were smooth and no collapse was found. Fig. 3(c) shows the side-opening on a HC-PCF whose outer diameter was 3.076 μm. In order to figure out whether the microchannel was connected to the inside and outside of the HC-PCF, the end face of the HC-PCF was also sectioned by FIB. As shown in Fig. 3(d), it was found that there was an approximately 0.7 μm × 0.7 μm hole on the core region. The total milling time per hole was about 8.5 min. By this way, the loss introduced by each microchannel was about 0.1~0.26 dB at a wavelength of 1550 nm, which successfully controls the transmission loss introduced by the microchannels to an acceptable low level.

For the selection of the hole spacing, this paper took a 1-meter-long HC-PCF as an example to model and simulate the gas diffusion process. Obviously, when the microchannels are uniformly distributed along the HC-PCF, the time required for the gas to completely diffuse into the hollow core region is the shortest. In this study, the gas diffusion process was simulated through the Transport of Diluted Species (tds) interface in COMSOL Multiphysics. It was obtained that when the distance between the adjacent microchannels was 20 cm, 10 cm or 5 cm, the gas diffusion saturation time was 589 s, 154 s or 45 s, respectively. Taking into account the ease of operation of the FIB equipment, the gas diffusion saturation time and the total losses of multiple microchannels, for a 1-meter-long HC-PCF and microchannels with the above-mentioned size, better detection performance can be achieved by keeping the hole spacing at 20 cm.

4. Optimal parameters determination

For the fiber loop cavity shown in Fig. 1(a), there is a 2 × 2 coupler with a splitting ratio of k_3 ($0< k_3<1$). Since the first beam of laser pulse collected by the photodetector does not pass through the absorption gas cell, it does not contain any gas absorption loss. While starting from the second beam of laser pulse, laser pulses pass through the absorption gas cell at least once, and therefore contains gas absorption loss to some degree. Thus, attention should be paid to the second and subsequent laser pulses. The intensity of the m^{th} laser pulse ($m\geq 2$) measured by the photodetector is:

$$I_m = I_0(1-k_3)^2 k_3^{m-2} 10^{-(m-1)(\beta_1+\beta_2)/10} \quad (8)$$

Where β_1 is the inherent loss of the fiber loop, dB; and β_2 is the gas absorption loss, dB.

According to the Eq. (8), the splitter ratio of the coupler has a great impact on the amplitude of the laser pulse sequence, which in turn affects the detection accuracy of the FLRDS system. It is not advisable for the amplitude difference between two adjacent laser pulses to be too large due to the splitting ratio of the coupler. This will cause the laser pulse to decay too fast, and only a small amount of gas absorption loss is

included in the total attenuation loss. At the same time, the amplitude of the laser pulse sequence should not be too low, resulting in inaccurate collection of small signals and excessive fitting errors. Therefore, both the number and intensity of pulse's peak should be considered.

In order to further determine the optimal coupler splitting ratio, this paper also discussed the influence of the coupler splitting ratio on the sensitivity of the FLRDS system. In this paper, the sensitivity of the FLRDS system is defined as the change in the ringdown time τ caused by the change in the target gas concentration C. The sensitivity of the FLRDS system can be expressed as:

$$\left|\frac{d\tau(\lambda_1)}{dC}\right| = \frac{\alpha L}{t_r} \Big/ \left(\frac{\alpha L}{t_r}\cdot C + \frac{1}{\tau(\lambda_2)}\right)^2 \tag{9}$$

In Eq. (9), the splitting ratio of the coupler will affect the ringdown time, which in turn affects the sensitivity of the FLRDS system. Nowadays, couplers with splitting ratios of 50:50, 75:25, 90:10, 99:1 are commercially available. In this paper, couplers with above four different splitting ratios were used to simulate the peak intensities of ringdown signals and the sensitivity of the system. The theoretical calculation result is shown in Fig. 4.

It can be seen from Fig. 4(a) that as the splitting ratio of the coupler increases, the amplitude of the laser pulse signal decreases. When the splitting ratio is 50:50 or 75:25, the amplitude of adjacent laser pulses attenuates rapidly, and the loss caused by gas absorption accounts for a small proportion of the total loss. In this case, the gas concentration information cannot be effectively obtained through the fitting of the ringdown curve and the calculation of the ringdown time. When the splitting ratio is 99:1, the overall laser pulse sequence amplitude is very small, tiny pulse signals are easily drowned in noise and the signal-to-noise ratio is poor. This makes it difficult to read the peak intensities through the oscilloscope accurately, which will result in large errors and poor accuracy.

It can be seen from Eq. (9) that the sensitivity of the system is inversely proportional to the gas concentration, so the sensitivity of the system decreases when the gas concentration increases. It can be known from Fig. 4(b) that when the splitting ratio is 90:10, among four different splitting ratios, the sensitivity of the FLRDS system is second to that when the splitting ratio is 99:1. Moreover, when the splitting ratio is 90:10, the decrease rate in sensitivity as the gas concentration increases is relatively slow. Therefore, in most cases for detecting dissolved acetylene in transformer oil, when the splitting ratio is 90:10, the sensitivity of the FLRDS system changes little with change of acetylene concentration.

To sum up, the coupler with a splitting ratio of 90:10 is more superior than others, and this splitting ratio will be used to carry out acetylene detection in this paper.

5. Results and discussion

5.1. Experimental verification of gas diffusion

According to the analysis of the influence of the optical topology on the performance of the detection system in Section 3 and Section 4, it can be seen that the optimal length of the HC-PCF in the FLRDS system should be 1 m, which can be suitable for detecting dissolved acetylene in transformer oil, and the detection system has the best overall performance. In this paper, to reduce the connection loss between the HC-PCF and SMFs, the two ends of fibers were fusion spliced. The total fusion splicing loss of the optical fiber at the wavelength of 1550 nm was about 3.01 dB. However, there was a loss of HC-PCF length in the fiber fusion splicing process, and the actual length of the HC-PCF in the proposed FLRDS system was 0.83 m.

Therefore, the above-mentioned 0.83 m-long HC-PCF was used as a gas cell and looped to a diameter of 5 cm. Both ends of the HC-PCF were spliced to conventional SMFs. In order to shorten the gas diffusion time, 4 microchannels were drilled on the side of the HC-PCF by FIB and separated from each other by 21 cm along the HC-PCF. The total loss caused by the introduction of the microchannels was about 0.52 dB. In order to verify whether the introduction of microchannels really shortens the response time of the system, this paper first injected 1500 ppm acetylene into the chamber to observe the gas diffusion saturation time. The gas diffusion saturation time of the developed sensing head was obtained by measuring the change in light transmittance. The gas diffusion sensing system is shown in Fig. 5(a). The experimental result of the gas diffusion time for the developed sensing head is shown in Fig. 5(b). The gas diffusion time required for fully diffuse into the HC-PCF's hollow core region was about 654 s. Moreover, based on Eq. (7), the theoretical gas diffusion saturation time is about 570 s. The possible reason for this small difference is that the wall effect cannot be ignored in the gas diffusion process for a HC-PCF.

5.2. FLRDS detection

FLRDS sensing system was set up as Fig. 6. And the structure parameter settings of the system were the same as the optimal parameter settings in Section 4. A tunable laser source (TSL-710, SANTEC CORPORATION) was used to output lasers with different wavelengths. An acoustic optical modulator (Gooch & Housego) was used to modulate the continue-wave laser into pulse form with a pulse width of 2 μs, a rising edge of 15 ns, a falling edge of 15 ns, and a frequency of 1 Hz. The processed HC-PCF mentioned above was sealed in a gas chamber filled with target gas, and a delay fiber (3 km long) was used to distinguish each pulse signal. Moreover, an amplifier was introduced to the proposed system to amplify the detected pulse signals. This is because the amplitude of the first optical pulsed signal detected by the photodetector is much larger than the second one due to the optical attenuation introduced by the coupler and the connection loss between the HC-PCF

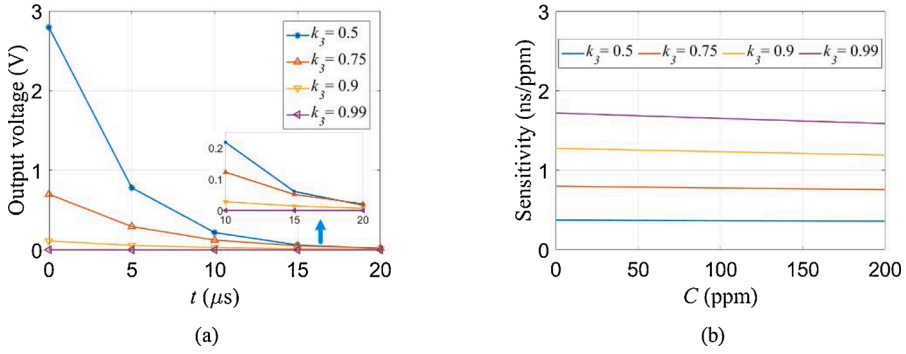

Fig. 4. (a) Simulation result of ringdown signal, (b) Simulation result of sensitivity.

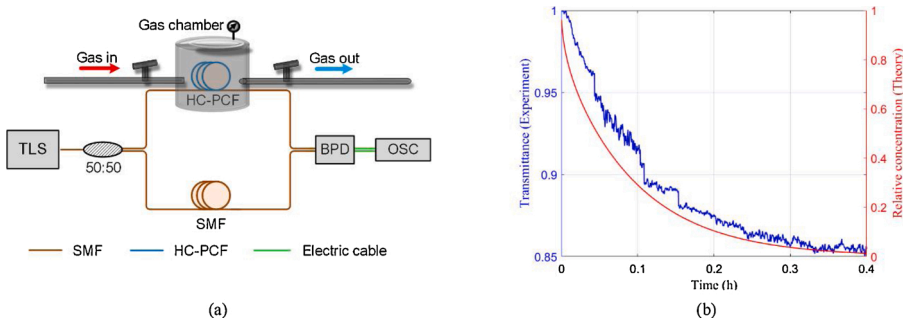

Fig. 5. (a) Schematic diagram of the platform for gas diffusion verification, (b) theoretical and experimental results of gas diffusion time. TLS: tunable laser source, BPD: balanced photodetector, OSC: oscilloscope.

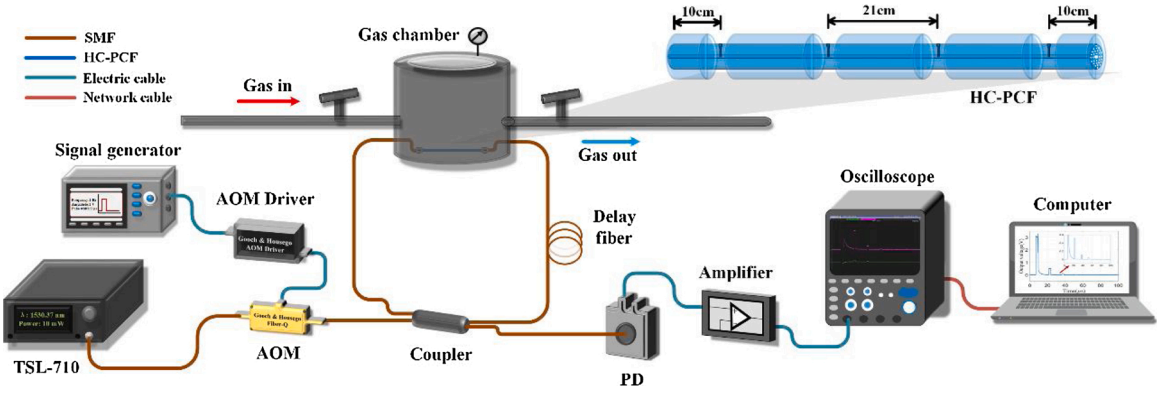

Fig. 6. Schematic diagram of FLRDS system.

and SMFs. In consequence, it is difficult to obtain a sufficient number of pulsed signals from the oscilloscope and figure out ringdown time accurately since it is difficult to avoid the first pulse signal on the oscilloscope by trigger settings. Thus, an alternative way to solve the above problem is to amplify the subsequent small signals for more pulse peak numbers and greater pulse peak intensity.

The amplifier is integrated on a PCB board, and the model of the amplifier chip is THS3091 (TEXAS INSTRUMENTS), and the gain of amplifier G is equal to 20.78. By applying the amplifier, the amplitudes of pulsed signals were significantly greater than that without the introduction of the amplifier. Also, the effective number of pulse's peak was increased from two to six. Due to the first pulse does not pass through the fiber loop, its amplitude is significantly larger than other ringdown peak signals passing through the gas cell. The existence of high-amplitude signals does harm to reading the amplitude of small signals on the oscilloscope, which is undesirable to data processing. In turn, this will reduce the accuracy of the detection results. However, since the first high-amplitude pulse signal does not pass through the gas cell and does not contain gas absorption information, it can be removed or clipped by circuit design. This paper introduced a feedback loop and MOS tube into the amplifier to cut the top of the high-amplitude pulse, and successfully achieved the effect of reducing the amplitude of the first pulse. By this way, the signal-to-noise ratio gets greatly improved, which is conducive to the accurate reading of other pulse signals. Therefore, the introduction of the amplifier can make help to the accurate fitting of the ringdown curve and the acquisition of the ringdown time.

To prove that the FLRDS system can be used to detect low-concentration acetylene in transformer oil, a series of trace acetylene detection were performed. Before gas detection, a series of gas samples of acetylene and nitrogen with different concentrations were prepared. The prepared gas samples with the concentration of 0, 9.97, 19.97, 29.95, 39.93, 49.99, 99.69, 199.67 ppm (room temperature, 101 kPa) were filled into the gas chamber in turn, and the trace acetylene detection were performed after the gas has completely diffused into the core region of the HC-PCF.

According to the spectrum data from HITRAN and PNNL databases, lasers with the wavelengths of 1530.37 nm (sensing laser, λ_1) and 1529.54 nm (reference laser, λ_2) were used to detect acetylene. At the central absorption wavelength of 1530.37 nm, the absorption line intensities of other characteristic gases (CH_4, C_2H_4, C_2H_6, CO, CO_2, H_2O, H_2) are much weaker than that of acetylene. At the central reference wavelength of 1529.54 nm, the absorption intensity of each characteristic gas is very weak. Also, the authors have experimentally proved that the above-mentioned center wavelength selection scheme can effectively avoid the cross-sensitivity problem in the previous research based on a TDLAS gas sensing system [9]. Impurities do not affect acetylene detection. Therefore, it is convincing that selecting the lasers with the wavelengths of 1530.37 nm (sensing laser, λ_1) and 1529.54 nm (reference laser, λ_2) can avoid the problem of cross-sensitivity.

During data processing, this paper selected 4 effective ringdown pulses for fitting, and the equivalent absorption optical path was about 3.32 m at this time. The differences between the two-wavelength ringdown times measured under different concentrations of C_2H_2/N_2 mixed gas are shown in Fig. 7.

The fitted equation representing the relationship between the differences of ringdown coefficients at dual wavelengths and the concentrations of acetylene was:

$$\frac{1}{\tau(\lambda_1)} - \frac{1}{\tau(\lambda_2)} = 0.000006706 \bullet C(C_2H_2) + 0.00002406 \quad (10)$$

The linear correlation coefficient R-square was about 0.9983. From Fig. 7 and the fitting Eq. (10), it can be seen that the acetylene concentration and differences of ringdown coefficients at dual wavelengths has a good linear relationship. The acetylene concentration can be back-calculated using the measurement results based on the quantitative relationship.

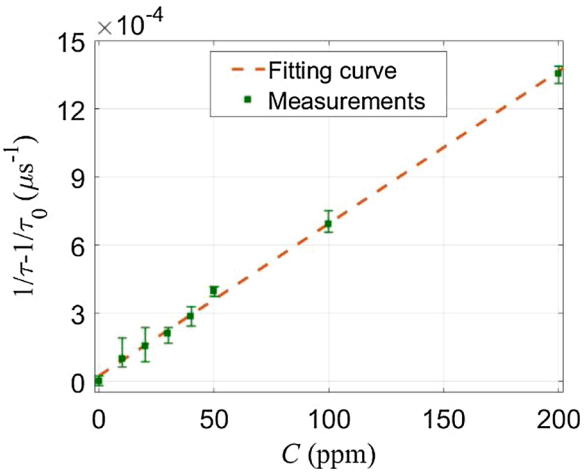

Fig. 7. Relationship between gas concentration and the difference of ringdown coefficients.

In order to determine the MDL of the FLRDS system, it is necessary to satisfy that the differences of ringdown time at dual wavelengths can be resolved by the oscilloscope. The average value of the ringdown time detected at the reference laser wavelength of 1529.54 nm was 11.2123 μs, and the standard deviation σ was 0.5176 μs. The MDL in terms of 1σ noise equivalent concentration [7] can be estimated to be 0.71 ppm. Such MDL can meet the detection of dissolved acetylene in transformer oil. As the sampling rate of the oscilloscope is 2.5 GS/s, considering the thrice standard deviation of the ringdown time, the precision of the proposed FLRDS system should satisfy:

$$[\tau(\lambda_2) \pm 3\sigma] - 1 \Big/ \left(\frac{\alpha l}{t_r} \cdot C + \frac{1}{\tau(\lambda_2) \pm 3\sigma}\right) \geq \frac{1}{2.5 \times 10^9} \tag{11}$$

Therefore, the precision of the proposed FLRDS system could reach 0.64 ppm. And according to the Eq. (9), the sensitivity of the proposed FLRDS system was about 1.0291 ns/ppm within the tested concentration.

To further verify the stability and the repeatability of the proposed FLRDS system, this paper conducted multiple experiments to observe the deviation of each detection result. When the C_2H_2 concentration was 200 ppm, the measured results of ten sets of data are shown in Fig. 8(a). The standard deviation was 2.87 ppm, and the relative standard deviation was 1.44 %. Recommendations to have accuracies better than ±15 % on DGA results to avoid misidentification of faults can be found in IEEE Std C57.104-2019. Therefore, the FLRDS system successfully meets this requirement. What is more, the volume fraction often mentioned in the detection standards refers to the volume fraction of gas molecules in transformer oil. When the detection results in the gas phase obtained in this paper are converted to condition in oil phase, the standard deviation is only 2.07 ppm.

In order to verify the insensitivity of the proposed FLRDS system to the fluctuation in the output power of the laser source, only the output power got changed. The fluctuation of the output power of the laser source in actual use is mostly between ±1 mW. To discuss special cases, the detection stability of the sensor when the fluctuation of the output power is ±2 mW was discussed in this paper. This paper detected the ringdown signals when the output power was different. The output power was 9.6 mW, 9.7 mW, 9.8 mW, 9.9 mW, and 10.0 mW in sequence. The detection results under different output powers are shown in Fig. 8(b). It can be seen that when the output power of the laser source was different, the fluctuation of the calculated concentration was very small, and the standard deviation was 2.21 ppm. Similar to the above discussion, when the detection results in the gas phase obtained in this paper are converted to condition in oil phase, the standard deviation is only 1.59 ppm. This verifies the superiority of the proposed FLRDS system in avoiding the influence of the instability of the laser source.

There are some other reported FLRDS-based gas sensing systems, the specific performances of the new proposed FLRDS system are compared with those systems, which is shown in Table 1. It should be noted that, due to the low concentration of the gas to be detected, the detection is difficult, and the relative detection error will be relatively large.

The total absorption pathlength is equal to the length of the gas cell multiplied by the number of effective ringdown peaks.

Based on the above experiments, the proposed FLRDS system has the advantages of fast response, high sensitivity, low detection limit, high accuracy, and low fluctuation. It can be effectively used for monitoring dissolved acetylene in transformer oil. What is more, the FLRDS system proposed in this paper is also suitable for the detection of other dissolved hydrocarbon gases in transformer oil. It is only necessary to select the suitable gas absorption spectrum accordingly and change the output laser wavelengths from the laser source to perform the detection.

6. Conclusion

This paper proposed a novel FLRDS gas sensing system based on HC-PCF for trace acetylene detection. A 0.83 m-long HC-PCF was used as a gas cell, and four microchannels were fabricated along it by focused ion beam processing technique. The gas diffusion saturation time was about 654 s and was great shorter than that of conventional DGA method, which provided an excellent time response performance. By adopting dual-wavelength method, the effective absorption pathlength increased several times (about 3.32 m), and the influence of inherent loss changes and the instability of photoelectric instruments on the detection results was effectively suppressed. Subsequently, trace acetylene sensing was carried out, and the results showed that the detection system has a minimum detection limit of 0.71 ppm and a detection precision of 0.64 ppm. The system's performance can meet the requirements of

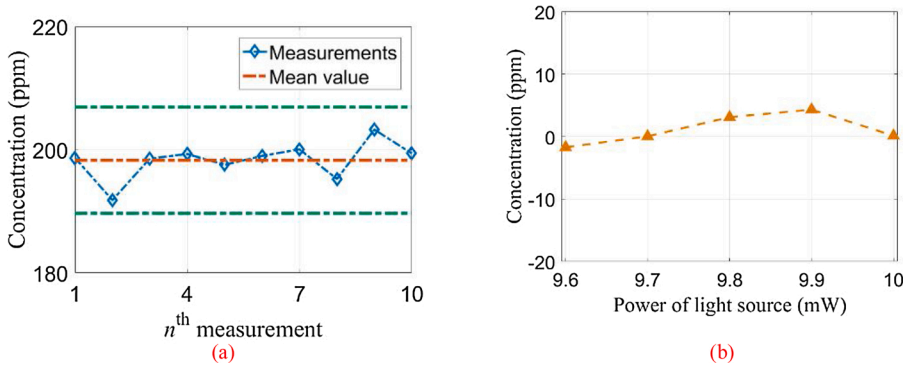

Fig. 8. (a) Experiment curve of fluctuation measurement when the acetylene concentration was 200 ppm; (b) Measurement results when the output power of laser source is different when the acetylene concentration is 0 ppm.

Table 1
Specific performances' comparison of different sensors.

Technique	Target gas	Sensor structure	Total absorption pathlength	Detection range	Measurement error
Direct absorption FLRDS [15]	C_2H_2	not mentioned	25 cm	0–0.5 %	2.4 %
Direct absorption FLRDS [29]	CH_4	collimators	20 cm	not mentioned	3.0 %
Dual-wavelength differential absorption FLRDS [20]	C_2H_2	collimators	58.5 cm	0–5 %	0.4 %
Dual-wavelength differential absorption FLRDS [33]	CO_2	collimators	75 cm	not mentioned	not mentioned
Dual-wavelength differential absorption FLRDS [this paper]	C_2H_2	HC-PCF	332 cm	0–200ppm	1.44 %

detecting dissolved acetylene in transformer oil. The newly designed FLRDS gas sensing system provides a new detection idea for monitoring the acetylene dissolved in transformer oil.

CRediT authorship contribution statement

Yuan Wang: Design, Gas System design and setup, Measurement, Data analysis, Writing- Original Draft, discussion. **Guo-ming Ma:** Gas system design, Formal analysis, Project administration, Funding acquisition, Supervision, Discussion, Writing- Reviewing and Editing. **Diya Zheng:** Measurement, Data curation, Formal analysis, Software, Visualization, Writing- Reviewing and Editing. **Wei-qi Qin:** Electrical system setup, Discussion, Visualization, Writing- Reviewing. **Jun Jiang:** Investigation, Concept forming, Discussion, Writing- Reviewing and Editing. **Hong-yang Zhou:** Formal analysis, Visualization, Discussion, Writing- Reviewing. **Chao Yan:** Gas system design, Discussion, Writing-Reviewing and Editing.

Declaration of Competing Interest

The authors declare that they have no known competing financial interests or personal relationships that could have appeared to influence the work reported in this paper.

Acknowledgments

This work was supported by National Natural Science Foundation of China (51677070, 51977075, 51807088), Young Elite Scientists Sponsorship Program by CASTYESS20160004, Fok Ying-Tong Education Foundation for Young Teachers in the Higher Education Institutions of China (161053), Beijing Natural Science Foundation (3182036), the Fundamental Research Funds for the Central Universities (2019MS006), and the State Key Laboratory of Alternate Electrical Power System with Renewable Energy Sources (LAPS21001).

References

[1] G. Ma, Y. Wang, W. Qin, et al., Optical sensors for power transformer monitoring: a review, High Volt. 6 (2021) 367–386.
[2] T. Chu, P. Wang, C. Zhu, Modeling of active fiber loop ring-down spectroscopy considering gain saturation behavior of EDFA, J. Light. Technol. 38 (4) (2020) 966–973.
[3] H.-y. Zhou, et al., Optical sensing in condition monitoring of gas insulated apparatus: a review, High Volt. 4 (4) (2019) 259–270.
[4] J. Jiang, et al., Multi-gas detection in power transformer oil based on tunable diode laser absorption spectrum, IEEE Trans. Dielectr. Electr. Insul. 26 (1) (2019) 153–161.
[5] W. Chen, J. Wang, F. Wan, P. Wang, Review of optical fibre sensors for electrical equipment characteristic state parameters detection, High Volt. 4 (4) (2019) 271–281.
[6] J. Hodgkinson, R.P. Tatam, Optical gas sensing: a review, Meas. Sci. Technol. 24 (1) (2012) 012004.
[7] W. Jin, Y. Cao, F. Yang, H.L. Ho, Ultra-sensitive all-fibre photothermal spectroscopy with large dynamic range, Nat. Commun. 6 (2015) 6767.
[8] Q. He, C. Zheng, H. Liu, Y. Wang, F. Tittel, A Near-Infrared Gas Sensor System Based on Tunable Laser Absorption Spectroscopy and its Application in CH4/C2H2 Detection (SPIE OPTO), SPIE, 2017.
[9] G.-m. Ma, et al., Tracing acetylene dissolved in transformer oil by tunable diode laser absorption spectrum, Sci. Rep. 7 (1) (2017) 14961.
[10] Y. Zhao, L. Bai, B. Han, Q. Wang, Review on advances of sensors based on fiber loop ring-down spectroscopy, Instrum. Sci. Technol. 41 (4) (2013) 349–364.
[11] H. Waechter, J. Litman, A.H. Cheung, J.A. Barnes, H.-P. Loock, Chemical sensing using fiber cavity ring-down spectroscopy, Sensors 10 (3) (2010) 1716–1742.
[12] C. Wang, Fiber loop ringdown—A time-domain sensing technique for multi-function fiber optic sensor platforms: current status and design perspectives, Sensors 9 (10) (2009) 7595–7621.
[13] A. O'Keefe, D.A. Deacon, Cavity ring-down optical spectrometer for absorption measurements using pulsed laser sources, Rev. Sci. Instrum. 59 (12) (1988) 2544–2551.
[14] G. Stewart, K. Atherton, H. Yu, B. Culshaw, An investigation of an optical fibre amplifier loop for intra-cavity and ring-down cavity loss measurements, Meas. Sci. Technol. 12 (7) (2001) 843.
[15] Y. Zhao, L. Bai, Q. Wang, Gas concentration sensor based on fiber loop ring-down spectroscopy, Opt. Commun. 309 (2013) 328–332.
[16] Q. Zhang, J. Chang, Q. Wang, Z. Wang, F. Wang, Z. Qin, Acousto-optic Q-switched fiber laser-based intra-cavity photoacoustic spectroscopy for trace gas detection, Sensors 18 (1) (2018) 42.
[17] Y. Hoo, S. Liu, H.L. Ho, W. Jin, Fast response microstructured optical fiber methane sensor with multiple side-openings, IEEE Photonics Technol. Lett. 22 (5) (2010) 296–298.
[18] Y. Tan, W. Jin, F. Yang, Y. Jiang, H.L. Ho, Cavity-enhanced photothermal gas detection with a hollow fiber Fabry-Perot absorption cell, J. Light. Technol. 37 (17) (2019) 4222–4228.
[19] Y. Tan, W. Jin, F. Yang, H.L. Ho, High finesse hollow-core fiber resonating cavity for high sensitivity gas sensing application, 2017 25th Optical Fiber Sensors Conference (OFS) (2017) 1–4.
[20] Y. Zhao, et al., Novel gas sensor combined active fiber loop ring-down and dual wavelengths differential absorption method, Opt. Express 22 (9) (2014) 11244–11253.
[21] X. Qian, Y. Zhao, Y.-n. Zhang, Q. Wang, Theoretical research of gas sensing method based on photonic crystal cavity and fiber loop ring-down technique, Sens. Actuators B Chem. 228 (2016) 665–672.
[22] W. Yan, Q. Han, Y. Chen, H. Song, X. Tang, T. Liu, Fiber-loop ring-down interrogated refractive index sensor based on an SNS fiber structure, Sens. Actuators B Chem. 255 (2018), pp. 2018-2022, 2018/02/01.
[23] X. Yang, L. Duan, H. Zhang, Y. Lu, G. Wang, J. Yao, Highly sensitive dual-wavelength fiber ring laser sensor for the low concentration gas detection, Sens. Actuators B Chem. 296 (2019) 126637.
[24] T. Brauers, M. Hausmann, U. Brandenburger, H.-P. Dorn, Improvement of differential optical absorption spectroscopy with a multichannel scanning technique, Appl. Opt. 34 (21) (1995) 4472–4479.
[25] J.R. Chen, K. Numata, S.T. Wu, Error reduction methods for integrated-path differential-absorption lidar measurements, Opt. Express 20 (14) (2012) 15589–15609.
[26] J. Crank, The Mathematics of Diffusion, Oxford university press, 1979.
[27] Y. Hoo, W. Jin, H. Ho, J. Ju, D. Wang, Gas diffusion measurement using hollow-core photonic bandgap fiber, Sens. Actuators B Chem. 105 (2) (2005) 183–186.
[28] J.P. Carvalho, et al., Remote system for detection of low-levels of methane based on photonic crystal fibres and wavelength modulation spectroscopy, J. Sens. 2009 (2009).
[29] K. Yu, C. Wu, Z. Wang, Optical methane sensor based on a fiber loop at 1665 nm, IEEE Sens. J. 10 (3) (2010) 728–731.
[30] M. Amanzadeh, S.M. Aminossadati, A new approach for drilling lateral microchannels in photonic crystal fibres, in: 2016 IEEE Photonics Conference (IPC), IEEE, 2016, pp. 779–780.
[31] W. Yuan, F. Wang, O. Bang, Optical fiber sensors fabricated by the focused ion beam technique, in: International Society for Optics and PhotonicsOFS2012 22nd International Conference on Optical Fiber Sensors, vol. 8421, 2012, p. 842173.
[32] F. Wang, W. Yuan, O. Hansen, O. Bang, Selective filling of photonic crystal fibers using focused ion beam milled microchannels, Opt. Express 19 (18) (2011) 17585–17590.
[33] A. Yarai, K. Hara, Differential detection technique for fiber gas sensor based on cavity ring down spectroscopy, Procedia Eng. 120 (2015) 659–662.

Yuan Wang was born in Beijing municipality, China, in 1994. He received a B.S. degree in electrical engineering from North China Electric Power University, Beijing, China, in 2017. He is now pursuing a Ph.D. degree in electric engineering in North China Electric Power University, Beijing, China.

Guo-ming Ma (SM'18) was born in Hebei, China, in 1984. He received a B.S. degree in electrical engineering from North China Electric Power University (BAODING) in 2006. He received a Ph.D. degree in electrical engineering from North China Electric Power University (BEIJING) in 2011. He is a professor with the State Key Laboratory of Alternate Electrical Power System with Renewable Energy Source (North China Electric Power

University), Beijing, China. His research interests are condition monitoring of power apparatuses.

Diya Zheng was born in Hubei province, China, in 1996. She received a B.S. degree in electrical engineering and automation from Changsha University of Science and Technology (Changsha) in 2018. She is now working towards a master's degree in electrical engineering at North China Electric Power University, Beijing, China.

Wei-qi Qin was born in Liaoning province, China, in 1994. He received the B.S. degree in electrical engineering from North China Electric Power University, Beijing, China, in 2017. He is currently working toward the Ph.D. degree in electrical engineering with North China Electric Power University. His special fields of interest include condition monitoring and diagnosis of power transmission equipment, and optical fiber sensing technologies.

Jun Jiang was born in Anhui province, China, in 1988. He received a B.S. degree in electrical engineering and automation from China Agricultural University (CAU) in 2011. He received a Ph.D. degree in electrical engineering from North China Electric Power University (NCEPU, Beijing) in 2016. He is now working as an associate professor in the Department of Electric Engineering, Nanjing University of Aeronautics and Astronautics (NUAA), Nanjing, China. His research interests are condition monitoring of power apparatus and optical fiber sensing.

Hong-yang Zhou was born in Fujian province, China, in 1991. He received a B.S. degree in electrical engineering from North China Electric Power University, Beijing, China, in 2014. He received a Ph.D. degree in electrical engineering from North China Electric Power University (NCEPU, Beijing) in 2020. He is now working as a postdoctoral fellow in Tsinghua University. His research interests are condition monitoring of power apparatus and optical fiber sensing.

Chao Yan was born in Shanxi province, China, in 1989. He received a Ph.D. degree in chemistry from New Jersey Institute of Technology in 2018. He is a Postdoctoral Research Fellow in the Mechanical Aerospace Engineering Department of Princeton University, New Jersey, U.S. His research interests are optical diagnosis in structure and physical chemistry.